

# Filaggrin Polymorphisms and the Uptake of Chemicals through the Skin—A Human Experimental Study

Emelie Rietz Liljedahl,<sup>1</sup> Gunnar Johanson,<sup>2</sup> Helena Korres de Paula,<sup>1</sup> Moosa Faniband,<sup>1</sup> Eva Assarsson,<sup>1</sup> Margareta Littorin,<sup>1</sup> Malin Engfeldt,<sup>1</sup> Carola Lidén,<sup>2</sup> Anneli Julander,<sup>2</sup> Karin Wahlberg,<sup>1</sup> Christian Lindh,<sup>1</sup> and Karin Broberg<sup>1,3</sup>

<sup>1</sup>Division of Occupational and Environmental Medicine, Department of Laboratory Medicine, Lund University, Lund, Sweden

<sup>2</sup>Unit of Integrative Toxicology, Institute of Environmental Medicine, Karolinska Institutet, Stockholm, Sweden

<sup>3</sup>Unit of Metals and Health, Institute of Environmental Medicine, Karolinska Institutet, Stockholm, Sweden

**BACKGROUND:** The filaggrin protein is important for skin barrier structure and function. Loss-of-function (null) mutations in the filaggrin gene *FLG* may increase dermal absorption of chemicals.

**OBJECTIVE:** The objective of the study was to clarify if dermal absorption of chemicals differs depending on *FLG* genotype.

**METHOD:** We performed a quantitative real-time polymerase chain reaction (qPCR)-based genetic screen for loss-of-function mutations (*FLG* null) in 432 volunteers from the general population in southern Sweden and identified 28 *FLG* null carriers. In a dermal exposure experiment, we exposed 23 *FLG* null and 31 wild-type (wt) carriers to three organic compounds common in the environment: the polycyclic aromatic hydrocarbon pyrene, the pesticide pyrimethanil, and the ultraviolet-light absorber oxybenzone. We then used liquid-chromatography mass-spectrometry to measure the concentrations of these chemicals or their metabolites in the subjects' urine over 48 h following exposure. Furthermore, we used long-range PCR to measure *FLG* repeat copy number variants (CNV), and we performed population toxicokinetic analysis.

**RESULTS:** Lag times for the uptake and dermal absorption rate of the chemicals differed significantly between *FLG* null and wt carriers with low (20–22 repeats) and high *FLG* CNV (23–24 repeats). We found a dose-dependent effect on chemical absorption with increasing lag times by increasing CNV for both pyrimethanil and pyrene, and decreasing area under the urinary excretion rate curve ( $AUC_{(0-40h)}$ ) with increasing CNV for pyrimethanil. *FLG* null carriers excreted 18% and 110% more metabolite (estimated by  $AUC_{(0-40h)}$ ) for pyrimethanil than wt carriers with low and high CNV, respectively.

**CONCLUSION:** We conclude that *FLG* genotype influences the dermal absorption of some common chemicals. Overall, *FLG* null carriers were the most susceptible, with the shortest lag time and highest rate constants for skin absorption, and higher fractions of the applied dose excreted. Furthermore, our results indicate that low *FLG* CNV resulted in increased dermal absorption of chemicals. <https://doi.org/10.1289/EHP7310>

## Introduction

Exposure to chemicals on the skin can cause skin diseases, such as irritant and allergic contact dermatitis, urticaria, and skin cancer (Anderson and Meade 2014). Dermal exposure is also a risk factor for chemical-related systemic effects, such as asthma (Paggiaro et al. 1987; Petsonk et al. 2000; Redlich 2010) and nonskin cancers (Golka et al. 2012; Nakano et al. 2018). Most people are dermally exposed to chemicals on a daily basis from household products, cosmetics, agricultural pesticides, textile and leather articles, rubber and rubber chemicals, and air pollution (World Health Organization 2014). Household chemicals are often used without proper skin protection, and numerous hazardous chemicals in cosmetic products, including sunscreen, makeup, and hair dyes, are applied to the skin. Many individuals are also exposed to chemicals at work, and dermal exposure has been increasingly recognized as a major occupational health risk (Roskams et al. 2008).

The skin barrier protects against the absorption of these chemicals into the body. One important protein for the skin barrier structure is filaggrin (encoded by the filaggrin gene *FLG*), a 37-kDa protein present in the stratum corneum of the epidermis, the outmost layer of the skin. Profilaggrin (400 kDa) undergoes proteolysis into filaggrin monomers, which maintain the integrity

of the skin barrier and are further cleaved into amino acids, which function as natural moisturizing factors and help retain water in the skin (Sandilands et al. 2009).

*FLG* loss-of-function (null) mutations are common: approximately 2%–10% of Europeans carry at least one *FLG* null allele (Bandier et al. 2013; Brown et al. 2012; Greisenegger et al. 2010; Liljedahl et al. 2019; Wahlberg et al. 2019; Varbo et al. 2017). People who are homozygous for *FLG* null alleles lack filaggrin protein, and most have the disease ichthyosis vulgaris (Smith et al. 2006). People who are heterozygous have filaggrin deficiency in the skin (Smith et al. 2006). Human studies have found associations between *FLG* null alleles and increased risk of childhood atopic dermatitis (Palmer et al. 2006), occupational irritant contact dermatitis (Visser et al. 2013), allergic sensitization (van den Oord and Sheikh 2009), and allergic rhinitis (van den Oord and Sheikh 2009).

The *FLG* gene is composed of repetitive sequences with copy number variants (CNVs) consisting of 10, 11, or 12 copies of the sequence encoding filaggrin monomers. The *FLG* CNV genotype was positively associated with the amount of natural moisturizing factors in the skin and negatively associated with the risk of atopic dermatitis in a case–control study of Irish individuals (cases were children with a mean age of 3.3 y, controls were adults with a mean age of 36.2 y) (Brown et al. 2012). Cross-sectional studies showed an association between *FLG* null alleles and higher urinary levels of phthalates in Danish men (Joensen et al. 2014), and between higher *FLG* CNV and lower levels of polycyclic aromatic hydrocarbons (PAHs) in the urine of a sample of chimney sweeps (Wahlberg et al. 2019). Although these studies associated *FLG* null and certain CNV with higher internal chemical exposure, the link to dermal uptake could not be established. Protection of individuals with a high dermal absorption is important because dermal uptake is a major route of environmental exposure to chemicals. New chemicals are continuously being added to consumer products all over the world. Still, there is limited research on the role of genetics in dermal chemical exposure and absorption.

The aim of this study was to clarify whether variations in *FLG* influence the degree of dermal chemical uptake. For this

---

Address correspondence to Karin Broberg, Institute of Environmental Medicine (IMM), Box 210, 17177 Stockholm, Sweden. Email: [karin.broberg@ki.se](mailto:karin.broberg@ki.se)

Supplemental Material is available online (<https://doi.org/10.1289/EHP7310>).

The authors declare they have no actual or potential competing financial interests.

Received 24 April 2020; Revised 20 November 2020; Accepted 20 November 2020; Published 13 January 2021.

**Note to readers with disabilities:** *EHP* strives to ensure that all journal content is accessible to all readers. However, some figures and Supplemental Material published in *EHP* articles may not conform to 508 standards due to the complexity of the information being presented. If you need assistance accessing journal content, please contact [ehponline@niehs.nih.gov](mailto:ehponline@niehs.nih.gov). Our staff will work with you to assess and meet your accessibility needs within 3 working days.

purpose, we performed a controlled human exposure experiment in which we exposed *FLG* null carriers and homozygous wild-type (wt) controls to three different organic substances found in food, air, and/or cosmetics: pyrimethanil, which is a fungicide used in conventionally grown fruit; pyrene, a PAH produced by incomplete combustion of organic materials; and oxybenzone, used as an ultraviolet (UV) filter in sunscreen to protect the skin and as a UV absorber in other cosmetics, rubber, and numerous organic materials to protect the product. We then measured urinary exposure biomarkers using liquid-chromatography–tandem mass spectrometry (LC-MS/MS) and compared the levels of the chemicals or their metabolites and the toxicokinetics between *FLG* null carriers and wt carriers grouped according to *FLG* CNV genotype.

## Materials and Methods

### Chemicals

Acetone, ethanol, formic acid, pyrimethanil: 4,6-dimethyl-N-phenyl-2-pyrimidinamine (CAS 53112-28-0), pyrene (CAS 129-00-0), and its metabolite 1-hydroxy-pyrene (CAS 5315-79-7), were purchased from Sigma Aldrich; oxybenzone (2-Hydroxy-4-methoxyphenyl)-phenylmethanone (CAS 131-57-7; referred to as benzophenone-3 on cosmetics' ingredient lists and in EU Cosmetics Regulation); the pyrimethanil metabolite OH-pyrimethanil 4-[(4,6-dimethyl-2-pyrimidinyl) amino] phenol (CAS 81261-84-9); and the internal standards <sup>2</sup>H<sub>3</sub>-oxybenzone, <sup>2</sup>H<sub>4</sub>OH-pyrimethanil, and <sup>2</sup>H<sub>9</sub>-1-hydroxy-pyrene, were purchased from Toronto Research Chemicals. Acetonitrile (hyper grade), ammonium acetate, and methanol were from Merck. β-glucuronidase/arylsulfatase from *Helix pomatia* was purchased from Roche Diagnostics Scandinavia AB. Water was produced by Milli-Q® Integral 5 system, Millipore.

### Ethics

The study was approved by the Regional Ethics Committee in Lund, Sweden. The exposure doses used in this study were equal or below the acceptable daily intake (ADI, for pyrimethanil ≤0.17 mg/kg; according to [http://ec.europa.eu/health/ph\\_risk/committees/04\\_sccp/docs/sccp\\_o\\_159.pdf](http://ec.europa.eu/health/ph_risk/committees/04_sccp/docs/sccp_o_159.pdf)) or the tolerable daily intake (TDI, for pyrene 0.03 mg/kg according to [http://www.popstoolkit.com/tools/HHRA/TDI\\_USEPA.aspx](http://www.popstoolkit.com/tools/HHRA/TDI_USEPA.aspx); and for oxybenzone 6% of cosmetics according to [http://ec.europa.eu/health/ph\\_risk/committees/04\\_sccp/docs/sccp\\_o\\_159.pdf](http://ec.europa.eu/health/ph_risk/committees/04_sccp/docs/sccp_o_159.pdf)) levels for each chemical. Participants were given information about the purpose of the project, the type of chemicals that they were going to be exposed to, the type of samples that were going to be collected, and any risks of discomfort during sampling. They were informed about how the samples and personal data are stored and that they could withdraw their participation at any point during the study. They were informed that results from the study would be published on a group level. Each participant gave their written informed consent.

### Study Population and Recruitment, Phase I

In phase I, volunteers were recruited by advertising online and on billboards at different companies and university campuses in Lund and Malmö, Sweden. Inclusion criteria were that volunteers should be nonsmoking and above 18 years of age. Interested volunteers (*n* = 488) received information about the project and gave their informed consent (*n* = 445). Volunteers received a saliva sample collection kit (Oragene DNA OG-500 kit, DNA Genotek) and a questionnaire regarding nickel allergy (that will be published separately), smoking and snuff habits, as well as occupation. Saliva samples (*n* = 432) and questionnaires were sent by

regular mail service to the laboratory of Occupational and Environmental Medicine, Lund University, and stored at room temperature (RT) until DNA extraction was performed. A flow chart of the study is shown in Figure 1.

### DNA Extraction and Genotyping

DNA was extracted from saliva samples from the 432 volunteers using the prepIT•L2P extraction kit (DNA Genotek) according to the manufacturer's instructions. Genotyping of the most common *FLG* null mutations in Europeans (Brown and McLean 2012) was performed using TaqMan™ assays as described elsewhere (Liljedahl et al. 2019). The *FLG* null variants included in analyses were single nucleotide polymorphisms (SNPs) R501X, present in CNV repeat 1; R2447X, present in CNV repeat 7; and S3247X, present in CNV repeat 8<sup>2</sup> (all leading to a stop codon and a truncated protein); and the deletion mutation 2282del4, present in CNV repeat 1 (leading to a stop codon and a truncated protein). Primer and probe sequences are described in Table S1. The primers and probes were from Thermo Fisher Scientific. The final reaction of 5 μL contained TaqMan™ genotyping Master Mix (1 ×; Thermo Fisher), sterile water (Thermo Fisher), forward and reverse primers (900 nM), fluorescent probes (200 nM), and DNA (2 ng/μL). To improve specificity, two forward primers were used in the 2282del4 assay (Sandilands et al. 2007), where the inner primer was added to the reaction separately at a final concentration of 500 nM. Samples were run in 384-well plates on a real-time polymerase chain reaction (PCR) machine (7900HT, Applied Biosystems) with the following conditions: 95°C for 10 min; 45 cycles of 92°C for 15 s, and 60°C for 90 s (60 s for the 2282del4 assay).

### Recruitment, Phase II

*FLG* null allele carriers (*n* = 28) and an equal number of controls (noncarriers matched to carriers by age and sex) identified in phase I were contacted about continuing into the dermal exposure experiment (phase II). Four *FLG* null carriers turned down the request to participate further, and one did not attend on the day of the exposure experiment. Eight additional controls (of which six were women) were recruited to increase statistical power and to cover for potential dropouts. Participants in phase II are shown in Table 1.

### Exposure Experiment, including Sampling

A physician was always present during the dermal exposure experiment. To minimize background exposure of the selected

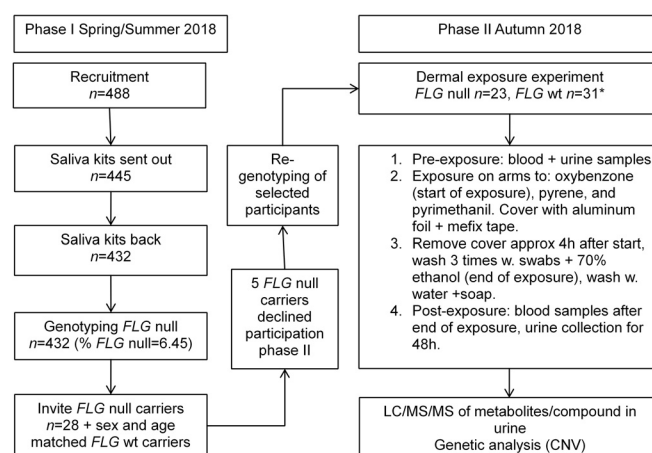


**Figure 1.** Flow chart of the two phases of the exposure experiment. Note: \*8 extra wt carriers were included.

**Table 1.** Characteristics, self-reported symptoms and diseases, and *FLG* null frequencies among the study participants.

Characteristic	n (%)		p-Value <sup>a</sup>
	<i>FLG</i> null (n = 23)	<i>FLG</i> wt (n = 31)	
Age (mean ± SD)	39.6 ± 15.0	38.8 ± 15.3	0.45
BMI (mean ± SD)	24.4 ± 5.8	24.1 ± 4.6	0.62
Sex			
Male	10 (43.5)	12 (38.7)	0.72
Female	13 (56.5)	19 (61.7)	—
Smoking			
Passive smoker	0 (0)	3 (9.7)	0.12
Party smoker	2 (8.7)	1 (3.2)	0.38
Previous smoker	8 (34.8)	9 (29.0)	0.57
Rash	4 (17.4)	7 (22.6)	0.64
Allergy symptoms, nose	14 (60.9)	12 (38.7)	0.20
Allergy symptoms, eyes	15 (65.2)	12 (38.7)	0.13
Asthma	4 (17.4)	3 (9.7)	0.40
Hand eczema	7 (30.4)	5 (16.1)	0.21
Wrist/forearm eczema	4 (17.4)	5 (16.1)	0.90
Dry skin	15 (65.2)	17 (54.8)	0.31
Childhood eczema	6 (26.1)	8 (25.8)	0.98
Nickel allergy	1 (4.3)	6 (19.4)	0.21
<i>FLG</i> null genotype			
R501X	8 (34.7)	0	NA
R2447X	2 (8.7)	0	NA
S3247X	3 (13.0)	0	NA
2282del4	10 (43.5)	0	NA

Note: p-Values represent differences between *FLG* null and wt carriers. —, no data; BMI, body mass index; SD, standard deviation; NA, not applicable.

<sup>a</sup>For continuous variables: Student's *t*-test, for categorical variables: chi-square test.

chemicals, participants were given instructions not to consume grapes, strawberries, or apples (to avoid pyrimethanil exposure); not to smoke cigarettes or eat grilled food (to avoid pyrene exposure); and not to use sunscreen or skin moisturizers (to avoid oxybenzone exposure) 2 d before until 2 d after the exposure experiment. The following samples were taken 10–30 min prior to the exposure: blood (two K<sub>2</sub>EDTA tubes, BD Vacutainer; one SST II Advance tube, BD Vacutainer; one PST II heparin tube, BD Vacutainer; one PAX tube, PreAnalytiX GmbH); and one spot urine (500 mL polypropylene bottle, translucent, with wide neck and screw cap, VWR). For the treatments, a solution containing 23.5 mg pyrimethanil/mL was prepared in ethanol, a 5-mg/mL solution of pyrene was prepared in 1:1 ethanol:acetone, and a 23.5-mg/mL solution of oxybenzone was prepared in ethanol. The exposure experiment went on for 2 months, so fresh solutions of each chemical were prepared weekly. An area along the bicep brachii of the right upper arm was marked for pyrimethanil (5 × 5 cm), on the volar aspect of the lower right arm for pyrene (5 × 10 cm), and along the bicep brachii of the upper left arm for oxybenzone (5 × 5 cm). Finally, 200 μL of each individual solution, oxybenzone (4.7 mg), pyrene (1.1 mg), and pyrimethanil (4.7 mg), was added to the marked areas in that order. The solution was spread out evenly with the pipette tip. The same dose was used for all study participants and was equal or below the ADI or the TDI levels for each chemical. The timing of the exposure was started when the oxybenzone solution had dried on the skin (by visual inspection). After drying, the exposed areas were covered with aluminum foil (Rio) and secured with adhesive dressing tape (Mefix, Mölnlycke Health Care). During the exposure, participants were allowed to have water, tea, coffee, or hot chocolate, but otherwise they fasted. Participants were exposed for 4 h, during which time they rested and answered an extensive questionnaire concerning, for example, asthma (“Have you ever had asthma?” and “If yes, did a physician make the diagnosis?”), allergies [“Have you ever had allergic symptoms from the nose (so-called hay fever) from for example pollen or animals?” and “Have you ever had allergic symptoms from the

eyes from for example pollen or animals?”], and eczema (“Have you ever had an itchy rash, occasionally over at least 6 months, in skin creases?”, “Have you ever had hand eczema?”, and “Did you have eczema when you were a child?”).

After 4 h of exposure, the aluminum foil and tape were removed from the participants' arms. The exposed areas were washed three times with cotton swabs wetted with 70% ethanol. Photographs of the arms were taken, and participants were asked to wash their arms with water and soap immediately. Blood samples were taken following the same procedure outlined above, and participants were given instructions, a cooler bag, and 16 500-mL bottles (VWR) to collect urine. Blood samples were kept at RT for 20 min, separated by centrifugation for 10 min at 2,200 × *g* into plasma and serum (not analyzed here), aliquoted in 2-mL screw-cap tubes (Eppendorf), and stored at –80°C. Blood intended for RNA analysis (not analyzed here) was kept at RT for 24 h and stored at –20°C. Whole blood and heparin tubes were stored at –20°C. Study participants collected full urine voids *ad libitum* in separate bottles during the exposure and for approximately 48 h post exposure. Urine samples were kept in a cooler bag at RT until they were delivered to the laboratory after the 48-h period, where they were stored at 5°C. The volume of each urine void was registered and 10-mL aliquots of each urine sample were taken and stored at –20°C.

### Re-Genotyping of Study Participants

All participants included in the phase II dermal experiment were genotyped a second time to confirm the genotyping in phase I. Pre-exposure blood samples were extracted using the Omega E.Z.N.A. kit (Omega Bio-tek) and genotyped for *FLG* null alleles as described above.

### CNV Analysis

CNV was determined according to a modified long-range PCR method originally described in Brown et al. 2012, in which amplification of the gene from repeat 7 results in different product sizes, depending on the CNV. The final reaction of 15 μL contained sterile water (Thermo Fisher), LaTaqMg<sup>2+</sup> buffer (10 ×; TaKaRa Bio), dNTPs (2.5 mM; TaKaRa Bio), forward and reverse primers (10 μM; forward primer 5'-CCCAGGACAAGCAGGAACT-3' and reverse primer 5'-CTGCACTACCATAGCTGCC-3'), TaKaRa polymerase (5 U/μL; TaKaRa Bio), and DNA (10 ng/μL). Amplification was performed on a PCR machine (T100 Thermal Cycler, Bio-Rad) with the following conditions: 94°C for 1 min, 30 cycles of 98°C for 10 s, 66°C for 30 s, and 72°C for 8 min, followed by a final extension step of 72°C for 10 min. Agarose gels (1% w/v) with GelRed (Biotum) were loaded with PCR product alongside a 1-kb Plus DNA ladder (Invitrogen). Sizes of the expected PCR products were 4,277 base pairs (bp) (repeats 7–10); 5,249 bp (repeats 7–11); and 6,224 bp (repeats 7–12). The presence or absence of the 12th repeat was confirmed by a predesigned assay (rs12730241 SNP assay, Thermo Fisher) according to the manufacturer's recommended protocols) and run according to *FLG* null genotypes. We were unable to identify the CNV of three wt carriers. The *FLG* wt participants were divided into two groups based on whether they had low CNV (defined as total CNV for both alleles of 20–22; combinations 10/10, 10/11, 11/11, 10/12) or high CNV (total CNV of 23–24; 11/12, 12/12). *FLG* null carriers were not grouped according to CNV because we did not assess which CNV corresponded to the functional allele and thus would be expressed.

### Analysis of Biomarkers in Urine

**Calibration standards and quality controls.** The exposure biomarkers analyzed in the urine were OH-pyrimethanil, oxybenzone,

and 1-hydroxy-pyrene. Stock solutions were prepared by accurately weighing the compounds in 10-mL flasks in duplicates and dissolving in methanol. A blank urine sample, obtained from a healthy volunteer at the lab and without detectable levels of the metabolites or chemicals in the study, was used to prepare the calibration standards. The chemical blanks were prepared in Milli-Q® water. For quality control samples, the blank urine sample was spiked with the three compounds to give final concentrations of 10 and 20 ng/mL for OH-pyrimethanil and oxybenzone, and 5 and 10 ng/mL for 1-hydroxy-pyrene. The quality control samples were stored at  $-20^{\circ}\text{C}$ .

### Sample Preparation for LC-MS/MS

The urine samples were thawed and vortexed, and 500  $\mu\text{L}$  of each sample was pipetted into a 2-mL 96-well plate (Alhmdow et al. 2017). For the calibration standards, 475  $\mu\text{L}$  of blank urine was spiked with 25  $\mu\text{L}$  of stock solutions containing the compounds. The calibration standards ranged from 2 to 1,800 ng/mL for OH-pyrimethanil, 1 to 900 ng/mL for oxybenzone, and 0.2 to 90 ng/mL for 1-hydroxy-pyrene. A set of calibration standards, several chemical blanks, and quality control samples were included in each 96-well plate. Then, 25  $\mu\text{L}$  of internal standard for all compounds, 10  $\mu\text{L}$   $\beta$ -glucuronidase/aryl-sulfatase enzyme, and 150  $\mu\text{L}$  of 1 M ammonium acetate buffer (pH 6.5) were added. The plates were covered with silicone mats (Sealing Mat, 96 square well; Kinesis), vortexed, and incubated overnight at  $37^{\circ}\text{C}$  with agitation at 400 rpm. The plates were stored at  $-20^{\circ}\text{C}$  until analysis. Before analysis, the samples were mixed and centrifuged at  $3,000 \times g$  for 10 min.

### LC-MS/MS Analysis

The urine samples were analyzed using liquid chromatography systems (UFLCRX, Shimadzu Corporation) coupled to triple quadrupole linear ion trap mass spectrometers (Sciex). Analysis of OH-pyrimethanil and oxybenzone were performed in positive ionization mode on a QTRAP® 5500 and 1-hydroxy-pyrene in negative ionization mode on a QTRAP® 6500+. The instrument settings and transitions for the quantifier and qualifier ions are shown in Table S2. All data acquisition and data processing were performed using Analyst® 1.6.3 (AB Sciex).

For OH-pyrimethanil, the chromatographic separation was performed on a Poroshell 120EC-C18 column ( $4.6 \times 100$  mm,  $2.7 \mu\text{m}$ ; Agilent Technologies). The mobile phases used were a) 0.1% formic acid in Milli-Q® water and b) 0.1% formic acid in methanol. The sample injection volume was 3  $\mu\text{L}$ , and the flow rate through the column was 0.7 mL/min. The column temperature was maintained at  $40^{\circ}\text{C}$ . The mobile phase gradient started with 50% mobile phase B, followed by a linear gradient to 95% at 2.2 min and equilibrated at 50% B for 2 min.

For oxybenzone, the chromatographic separation and the mobile phases were performed as for OH-pyrimethanil. The sample injection volume was 4  $\mu\text{L}$ , and the flow rate through the column was 0.4 mL/min. The column temperature was maintained at  $60^{\circ}\text{C}$ . The mobile phase gradient started with 75% mobile phase B, followed by a linear gradient to 95% at 2.0 min and equilibrated at 75% B for 2 min.

For 1-hydroxy-pyrene, the separation was performed on a Genesis Lightn C18 column ( $4.6 \times 2.1$  mm,  $4 \mu\text{m}$ ; Hichrom) with mobile phases consisting of a) Milli-Q® water and b) methanol. The sample injection volume was 5  $\mu\text{L}$ , and the flow rate through the column was 0.6 mL/min. The column temperature was maintained at  $60^{\circ}\text{C}$ . The mobile phase gradient started with 20% mobile phase B, followed by a linear gradient to 95% at 2.0 min and equilibrated at 20% B for 3 min.

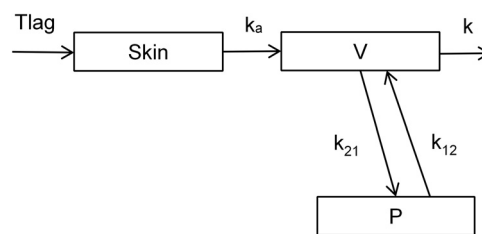


**Figure 2.** Compartmental model used in the toxicokinetic analysis: lag time for skin penetration ( $T_{\text{lag}}$ , h), first order skin absorption constant ( $k_a$ ,  $\text{h}^{-1}$ ), volume of central compartment ( $V$ , L), peripheral compartment ( $P$ ) first order transfer rate constants ( $k_{12}$  and  $k_{21}$ ,  $\text{h}^{-1}$ ), and first order elimination rate constant ( $k$ ,  $\text{h}^{-1}$ ).

The samples were analyzed in duplicates in 20 batches and each batch of samples contained a set of calibration standards, chemical blanks, and quality controls. The limit of detection (LOD) was 0.1 ng/mL for OH-pyrimethanil, 0.2 ng/mL for oxybenzone, and 0.2 ng/mL for 1-hydroxy-pyrene. The between-batch precision was determined by comparing duplicate analyses. The precisions are shown in Table S3, and the coefficients of variation were between 4% and 13%. The laboratory participates in the Erlangen interlaboratory comparison program for 1-hydroxy-pyrene and oxybenzone and fulfills the requirements. The laboratory also participates in the Interlaboratory Comparison Investigations (ICI) and External Quality Assurance Schemes (EQUAS) (ICI/EQUAS) exercises for the analysis of 1-hydroxy-pyrene and is approved in the HBM4EU project.

For pyrimethanil, the median concentration in pre-exposure urine samples was  $<\text{LOD}$  ng/mL (57%  $<\text{LOD}$ ) for *FLG* null carriers, and 0.4 ng/mL (35%  $<\text{LOD}$ ) for *FLG* wt carriers; for 1-hydroxy-pyrene, the median was  $<\text{LOD}$  ng/mL (96%  $<\text{LOD}$ ) for *FLG* null carriers, and  $<\text{LOD}$  ng/mL (90%  $<\text{LOD}$ ) for *FLG* wt carriers; and for oxybenzone, the median was 1.88 ng/mL (0%  $<\text{LOD}$ ) for *FLG* null carriers, and 4.45 ng/mL (6%  $<\text{LOD}$ ) for *FLG* wt carriers.

To adjust the biomarker levels for urinary dilution, the volume of each urine void was measured, and creatinine was analyzed at the Department of Clinical Chemistry, Lund University Hospital. The laboratory is accredited for creatinine analysis and is using an enzymatic colorimetric method (Mazzachi et al. 2000).

### Toxicokinetic Analyses

The fraction of the applied dose excreted (excreted dose across time) was estimated by calculating the area under the urinary excretion rate curve (AUC) by using the trapezoid method (Excel 2010; Microsoft). The end time for urine collection differed among the participants, so the AUC was calculated for 0–40 h. One *FLG* null carrier had only 5 urine samples with maximum sampling time 29 h after the exposure and had to be excluded from the AUC analysis. Subjects with pre-exposure baseline concentrations of test chemicals exceeding the levels achieved during exposure were also omitted from the analysis (one wt carrier for oxybenzone).

Dermal absorption and disposition were assessed by population toxicokinetic analysis. A three-compartment structural model representing skin and central and peripheral tissues was used (Figure 2). The skin compartment encompasses a lag time for skin penetration ( $T_{\text{lag}}$ ) and an absorption rate constant ( $k_a$ ). Urinary excretion from the central compartment was described by an elimination rate constant ( $k_e$ ), and exchange between the central and peripheral compartments was described by two rate constants ( $k_{12}$  and  $k_{21}$ ). All rate constants are first order.

The input data were the dermally applied dose (nmol) at time zero and the mid-time point (h) and the excretion rate (nmol/h) of each chemical in the urine samples. Subjects excluded from the AUC analysis were also excluded from the toxicokinetic analysis (one *FLG* null carrier and one wt carrier for oxybenzone). Numbers of subjects included *FLG* null: 22, and *FLG* wt: 30 (for oxybenzone) or 31 (for pyrimethanil and pyrene). When grouping the wt carriers according to CNV, subjects with an unknown CNV genotype were excluded from analysis (three wt carriers), and numbers of subjects included *FLG* wt CNV20–22: 19 (for oxybenzone) or 20 (for pyrimethanil and pyrene), and *FLG* wt CNV23–24: 8.

The software Monolix (version 2019R2; Lixoft) was used to estimate the model parameters. The built-in statistical model consists of an observation model and an individual model based on the structural toxicokinetic model. The observational model was set to a normal distribution, and a residual error model included in the observational model was used as proposed by the software after initial analysis. A lognormally distributed random effect was added to all model parameters. Correlations between parameters were accounted for if proposed by the software. The different genotypes (*FLG* null/wt, and *FLG* null/wt CNV20–22/wt CNV23–24) were entered as categorical covariates. The residual scatter plots for excretion rate and time were sufficiently evenly distributed around 0 (Figures S1–S3) and the observed vs. predicted plots were sufficiently evenly distributed around the line of unity (Figures S4–S6), altogether suggesting an adequate structural model.

### Statistical Analysis

Characteristics of the study participants, grouped by *FLG* null carriers and wt carriers, were compared by Student's *t*-test for continuous variables [age and body mass index (BMI)] and chi-square test for categorical variables (sex, smoking, rash, allergy with symptoms from nose/eyes, asthma, hand eczema, wrist/forearm eczema, dry skin, childhood eczema, and nickel allergy). The wt carriers were further divided into two subgroups based on their total CNV because we hypothesized that CNV affects skin barrier function but to a lesser extent than *FLG* null alleles. Categories were *FLG* null carriers, wt carriers with a total CNV of 20–22 (low CNV), and wt carriers with a total CNV of 23–24 (high CNV).

The  $AUC_{(0-40h)}$  was log transformed to improve normality. Differences in log  $AUC_{(0-40h)}$  depending on *FLG* null genotype were investigated using Student's *t*-test, and differences depending on *FLG* null and CNV genotype were investigated using analysis of variance (ANOVA) in SPSS (Statistics 25; IBM). Differences in log  $AUC_{(0-40h)}$  depending on *FLG* null genotype were further adjusted for age, BMI, and sex with ANOVA in SPSS (IBM).

Differences in estimated lag time, absorption rate constants and additional estimated parameters depending on *FLG* null genotype or on *FLG* null and CNV genotype were investigated using ANOVA in Monolix (Lixoft). To investigate whether other known factors were associated with toxicokinetic analysis parameters and thereby skin absorption of chemicals, additional covariates (age, BMI, and sex) were tested in the statistical model in Monolix (Lixoft).

## Results

### Characteristics of the Test Subjects

The characteristics of the *FLG* null carriers and the wt carriers did not differ significantly (Table 1). There were no significant differences in self-reported disease symptoms between the

groups, but *FLG* null carriers reported IgE-mediated allergies to a higher extent, with symptoms from the eyes and nose, asthma, and hand eczema, in comparison with the wt carriers.

The frequency of *FLG* null alleles was 6.5% in the entire study group (28 carriers out of 432), which was similar to that in other studies (Bandier et al. 2013; Brown et al. 2012; Greisenegger et al. 2010; Varbo et al. 2017). The distribution of the null mutations identified in the screening was 9 carriers (2.1%) for R501X, 3 (0.7%) for R2447X, 3 (0.7%) for S3247, and 13 (3.0%) for 2282del4. Of the participants with *FLG* wt, 20 had a total CNV of 20–22 (low CNV) and 8 had a total CNV of 23–24 (high CNV).

### Area under the Urinary Excretion Rate Curve ( $AUC_{(0-40h)}$ )

There were no statistically significant differences in mean  $AUC_{(0-40h)}$  for *FLG* null compared with wt carriers for any of the chemicals, but overall *FLG* null carriers excreted the highest fraction of the applied doses (Table S4). A similar trend was found in the analysis adjusted for BMI and age (sex was not associated,  $p > 0.52$ , with the  $AUC_{(0-40h)}$  for any of the chemicals and was not included in the final analysis), but it was not statistically significant (Table S5). When grouping wt carriers according to CNV, there was a significant negative association between log  $AUC_{(0-40h)}$  for pyrimethanil and *FLG* CNV genotype, with wt CNV20–22 having 15% smaller  $AUC_{(0-40h)}$  than *FLG* null and wt CNV 23–24 having 44% smaller  $AUC_{(0-40h)}$  than wt CNV20–22 to (Table 2). The same trend in  $AUC_{(0-40h)}$  between *FLG* genotype groups was found in the adjusted analysis (BMI and age), but it was not statistically significant ( $p = 0.095$ ) (Table S6). Pairwise comparison showed that there were significant differences between *FLG* null and wt CNV23–24 ( $p = 0.011$ , adjusted  $p = 0.037$ ) and between wt CNV20–22 and wt CNV23–24 ( $p = 0.048$ , adjusted  $p = 0.243$ ). No significant differences were seen for pyrene and oxybenzone, but for both chemicals, *FLG* null carriers showed the highest  $AUC_{(0-40h)}$  and *FLG* wt CNV23–24 carriers showed the lowest  $AUC_{(0-40h)}$  (Table 2; Table S6).

The variation in  $AUC_{(0-40h)}$  between individuals was large, with a factor of 20 between minimum (260 nmol) and maximum (5,111 nmol) values for pyrimethanil. The models with *FLG* genotype only showed  $R^2$  between 0.067–0.13 (Table 2) and the models with *FLG* genotype adjusted for age and BMI showed  $R^2$  between 0.26–0.29 (Table S6).

### Toxicokinetic Analysis

The observational data used for the toxicokinetic analyses is presented as excretion curves by *FLG* null and CNV genotype in Figure 3 and Figures S7–S8. *FLG* null carriers reached the highest excretion for pyrimethanil and oxybenzone (Figure 3 and Figure S7), whereas for pyrene the *FLG* wt CNV20–22 reached the highest excretion followed by *FLG* null and *FLG* wt with CNV23–24 (Figure S8). The lag times and dermal absorption rate constants by *FLG* null vs. wt carriers are presented in Table S4. For both pyrimethanil and pyrene, the mean lag time for dermal uptake was significantly shorter [62% (20 min) and 26% (20 min), respectively] among *FLG* null carriers compared with wt carriers. The lag time for oxybenzone was also shorter for *FLG* null carriers compared with wt carriers but not significantly different ( $p = 0.055$ ). Dermal absorption rate constants were significantly higher for *FLG* null compared with wt carriers for pyrimethanil and oxybenzone (18% and 32%, respectively), but not for pyrene.

When grouping the wt carriers by CNV (Table 2), the mean lag times for dermal uptake of pyrimethanil were significantly

**Table 2.** Area under the urine excretion rate curve ( $AUC_{(0-40h)}$ ), lag time for dermal absorption and dermal absorption rate constant by *FLG* null and CNV genotype.

Chemical	Genotype <sup>a</sup>	$AUC_{(0-40h)}$ (nmol, geometric mean; 95% CI)	<i>p</i> -Value (ANOVA)	Lag time (h, mean $\pm$ SD)	<i>p</i> -Value (ANOVA)	Absorption rate constant (h <sup>-1</sup> , mean $\pm$ SD)	<i>p</i> -Value (ANOVA)
Pyrimethanil	<i>FLG</i> null	1,676; 1,253, 2,243	0.038 <sup>b,c</sup>	0.14 $\pm$ 0.02	0.0001	0.19 $\pm$ 0.04	0.02
	<i>FLG</i> wt CNV20–22	1,421; 1,047, 1,927		0.37 $\pm$ 0.06		0.20 $\pm$ 0.05	
	<i>FLG</i> wt CNV23–24	799; 494, 1,294		0.66 $\pm$ 0.12		0.13 $\pm$ 0.03	
Pyrene	<i>FLG</i> null	28.4; 22.9, 35.1	0.195 <sup>d</sup>	0.91 $\pm$ 0.12	0.011	0.16 $\pm$ 0.05	0.019
	<i>FLG</i> wt CNV20–22	27.2; 21.8, 34.0		1.06 $\pm$ 0.16		0.14 $\pm$ 0.03	
	<i>FLG</i> wt CNV23–24	19.6; 13.8, 27.9		1.41 $\pm$ 0.29		0.11 $\pm$ 0.03	
Oxybenzone	<i>FLG</i> null	1,161; 891, 1,510	0.165 <sup>e</sup>	0.07 $\pm$ 0.01	0.000008	0.23 $\pm$ 0.07	0.0046
	<i>FLG</i> wt CNV20–22	1,061; 797, 1,409		0.04 $\pm$ 0.009		0.22 $\pm$ 0.08	
	<i>FLG</i> wt CNV23–24	711; 459, 1,104		0.23 $\pm$ 0.13		0.13 $\pm$ .04	

Note: *p*-Values for comparisons are between *FLG* null ( $n=22$ ), wt CNV20–22 ( $n$ [oxybenzone]=19,  $n$ [pyrimethanil and pyrene]=20), and wt CNV23–24 ( $n=8$ ). —, no data; ANOVA, analysis of variance; CI, confidence interval; CNV, copy number variants.

<sup>a</sup>Three participants do not have information about CNV.

<sup>b</sup>Significant pairwise comparison between *FLG* null and wt CNV23–24:  $P=0.011$ , and between wt CNV20–22 and wt CNV23–24:  $p=0.048$ .

<sup>c</sup> $R^2=0.13$ .

<sup>d</sup> $R^2=0.067$ .

<sup>e</sup> $R^2=0.075$ .

shorter [62% (14 min)] for *FLG* null carriers than for wt carriers with CNV20–22, and in turn, significantly shorter [79% (31 min)] than for wt carriers with CNV23–24. Examples of individual fits of the toxicokinetic model to excretion rate data for pyrimethanil are shown in Figure S9. Lag times for pyrene were significantly shorter for *FLG* null carriers than wt carriers with CNV20–22 and CNV23–24 [by 14% (9 min) and 35% (30 min), respectively]. Lag times for oxybenzone were similar for *FLG* null carriers and wt carriers with CNV20–22, but significantly shorter for *FLG* null carriers than wt carriers with CNV23–24 [by 69% (10 min)]. The mean dermal absorption rate constants were higher for pyrimethanil, pyrene, and oxybenzone for *FLG* null carriers than for wt carriers with CNV23–24 (by 50%, 45%, and 77% for each respective chemical), whereas wt carriers with CNV20–22 had absorption rate constants similar to those of *FLG* null carriers for all three chemicals (Table 2). Results from the analysis with additional covariates (age, BMI, and sex) did not change the significance level for the associations between lag time and absorption rate and *FLG* (Table S7).

Additional parameters (volume of the central compartment, rate constant from the central compartment to the peripheral compartment, rate constant from the peripheral compartment to the central compartment, and excretion rate constant) of the toxicokinetic model are presented in Tables S8–S9.

## Discussion

This is to the best of our knowledge the first study to establish the link between *FLG* genetics and differences in skin absorption of chemicals. Our results demonstrate that *FLG* variations can influence the rate at which chemicals are taken up through the skin as observed by differences in both the absorption rate constant and lag time between genotypes. We found that carriers of *FLG* null alleles had a shorter lag-time (significant for pyrimethanil and pyrene) and higher absorption rate (significant for pyrimethanil and oxybenzone) than *FLG* wt carriers, indicating that the *FLG* null mutations led to an impaired skin barrier and faster absorption. Our results further indicate that, in addition to *FLG* null alleles, a low *FLG* CNV may contribute to increased dermal uptake of the chemicals. Based on these findings, we propose that *FLG* null carriers and individuals with a low *FLG* CNV may constitute a group with increased susceptibility to chemical dermal absorption. Nevertheless, it should be noted that a large overall variation in chemical absorption (20-fold based on  $AUC_{(0-40h)}$ ) was observed between individuals in this study, and although some of the differences could be explained by *FLG*, there are likely

several other genes, as well as other factors, including biotransformation, contributing to the variation.

The chemicals included in this study are common among environmental, consumer, and occupational exposures. Pyrimethanil is a fungicide used in conventional fruit agriculture, and both workers and consumers can be exposed (Faniband et al. 2019). Pyrimethanil has been found to be an aryl hydrocarbon receptor agonist *in vitro* (Medjakovic et al. 2014) and has been shown to disrupt liver metabolism and thyroid hormones in rodents at high concentrations, 13–1,000 mg/kg/d (Hurley 1998). In humans, pyrimethanil is mainly metabolized by oxidation to OH-pyrimethanil, after which conjugation (mainly with sulfonate) occurs. After oral exposure, 80% of the compound was found in urine as OH-pyrimethanil (Faniband et al. 2019). Pyrimethanil is not considered of toxicological concern to humans below the ADI of 0.17 mg/kg/d and has low acute toxicity (<https://efsa.onlinelibrary.wiley.com/doi/pdf/10.2903/j.efsa.2006.61r>).

Pyrene is a PAH (not classifiable as to human carcinogenicity) (<https://echa.europa.eu/brief-profile/-/briefprofile/100.004.481>). Pyrene is metabolized by oxidation to 1-hydroxy-pyrene and excreted in urine both as free 1-hydroxy-pyrene and conjugated to sulfate or glutathione, and excreted in the bile in the conjugated form (Law et al. 1994; Saengtienchai et al. 2014). The metabolite 1-hydroxy-pyrene is frequently used as a marker for total exposure to PAHs (Ciarrocca et al. 2014). PAHs occur naturally as coal or crude oil or are produced by incomplete combustion of organic materials, and skin exposure occurs particularly in some occupations such as chimney sweeping (Kammer et al. 2011) and fire-fighting (Strandberg et al. 2018).

Oxybenzone (termed benzophenone-3 in cosmetic products) is a UV absorber used in various cosmetic products (Uter et al. 2014) for protection of skin and hair (referred to as a UV filter) and in other types of cosmetics and organic materials such as paint, rubber, and plastic products (referred to as a UV absorber). Dermal exposure to oxybenzone is very common (Han et al. 2016) and is largely attributed to the use of sunscreen. When administered to rats, urine was the main route of excretion. About 50% of what was found in urine was in the form of the parent compound, free, and conjugated with glucuronic acid (Okereke et al. 1993). In zebrafish, at a concentration of 84  $\mu$ g/L (10 times higher than the highest measured environmental level in water), oxybenzone exposure was associated with a decreased expression of estrogen receptor 1, androgen receptor, and cytochrome P450 aromatase B (Blüthgen et al. 2012). Among 215 Spanish men, there was a positive association between urinary oxybenzone levels and increased levels of follicle-stimulating

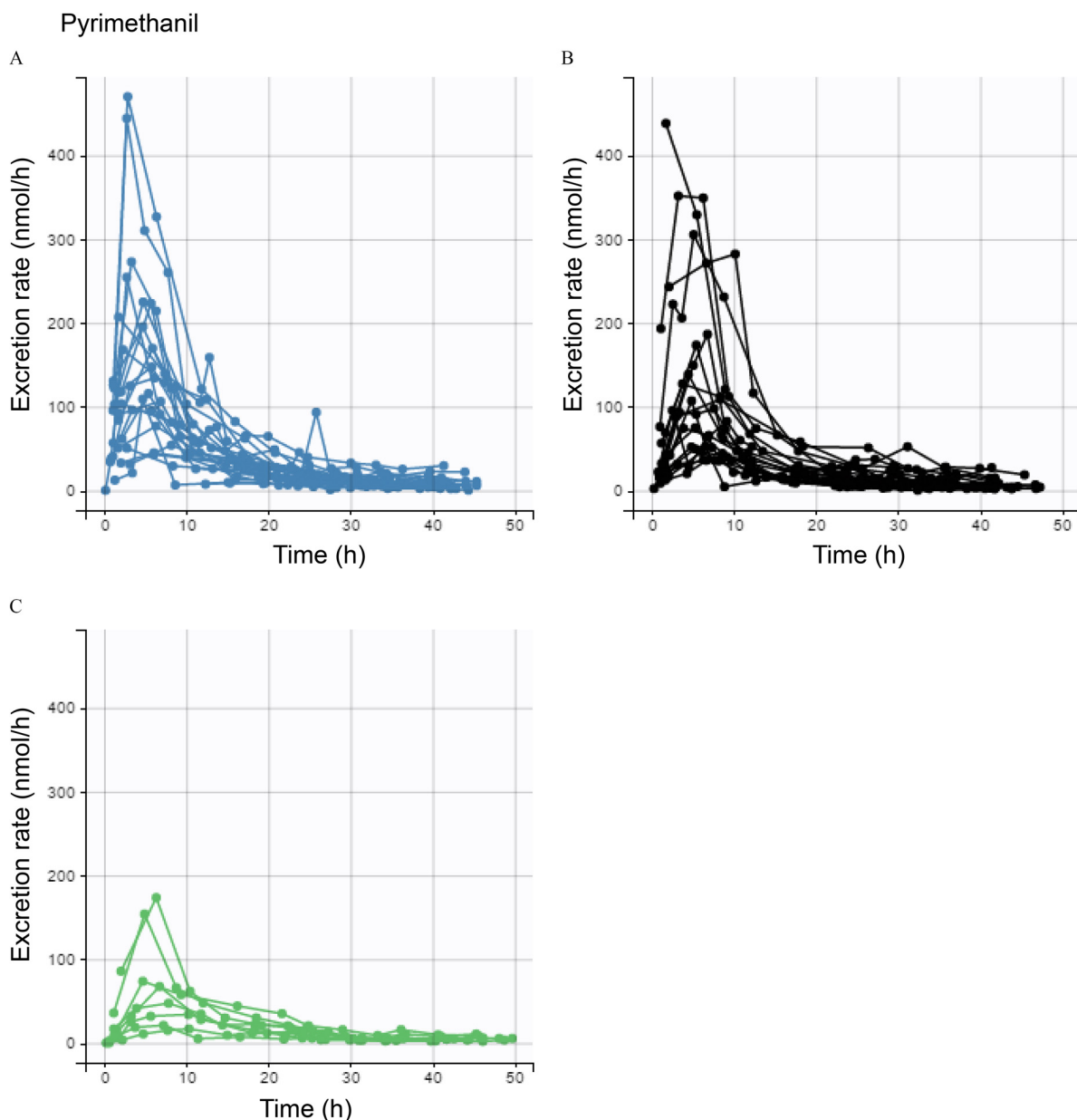


**Figure 3.** Excretion curves for pyrimethanil by FLG genotype. Each curve represents an individual. Excretion rates of (A) FLG null (blue) carriers, (B) wt carriers with CNV20–22 (black), and (C) wt carriers with CNV23–24 (green).

hormone (Adoamnei et al. 2018). Oxybenzone is under assessment as an endocrine disrupter by the Danish Environmental Protection Agency according to the European Chemical Agency (ECHA) (<https://echa.europa.eu/>), and has recently been found to affect fetal growth and sex ratio in mice (Santamaria et al. 2020). A Danish study of 65 male *FLG* null carriers and 130 male *FLG* wt carriers found slightly higher but only borderline significant levels of oxybenzone among *FLG* null carriers than among wt carriers (Joensen et al. 2017).

The three compounds used in this study have two aromatic rings or more and have similar molecular weights (pyrimethanil: 199.25 g/mol; pyrene: 202.25 g/mol; and oxybenzone: 228.24 g/mol). However, their lipophilicities differ widely, as indicated by their log octanol/water partition coefficients (log P) of 4.88 (pyrene) (PubChem 2004a), and 3.79 (oxybenzone) (PubChem 2004b) and 2.84 (pyrimethanil) (PubChem 2004c). For smaller molecular weight compounds, maximal solubility is

found for log P-values between  $-1$  and  $2$ , whereas  $\log P > 4$ , such as for pyrene, means a very high lipophilicity and a low solubility in skin (Casarett 2001; Nielsen et al. 2009). Potts and Guy proposed an equation predicting skin permeability of chemicals using log P and molecular weight (Potts and Guy 1992), according to which pyrene would be the slowest skin permeant, followed by oxybenzone and pyrimethanil. This prediction is reflected by the  $AUC_{(0-40h)}$  in our results, and partly by lag times and absorption rate constants where pyrene had the longest lag times and lowest rate constants, but followed by pyrimethanil and not oxybenzone as expected.

There are currently few studies of *FLG* CNV in relation to skin barrier function and chemical exposure. Brown et al. showed that higher CNV reduced the risk of atopic dermatitis in a dose-dependent manner, and resulted in higher levels of filaggrin breakdown products, indicating a beneficial influence on skin condition (Brown et al. 2012). In our previous studies, high CNV

(the presence of CNV12) among chimney sweeps was associated with lower levels of PAHs in urine (Wahlberg et al. 2019), and low CNV (the presence of CNV10) in hairdressers was associated with shorter telomeres (Liljedahl et al. 2019), indicating that a low CNV may contribute to higher uptake of chemicals and more systemic effects. Consistent with the studies mentioned above, we observed an increased uptake of chemicals in *FLG* wt carriers with lower total CNV (20–22 copies) compared with those with high CNV (23–24 copies). Due to the small number of individuals representing each CNV type, we could not gain enough statistical power to evaluate a potential dose effect on the uptake with decreasing CNV. Moreover, due to the lack of information regarding the DNA strand location of *FLG* null alleles in relation to the CNV genotype, we could not evaluate the influence of CNV in *FLG* null carriers. Indeed, it would be interesting to investigate whether a high CNV in the wt allele could to some degree compensate for the partial loss of functional *FLG* in heterozygotes carrying a wt allele and a *FLG* null allele. Low CNV is frequent in the European population (CNV10 allele frequency around 30%) (Brown et al. 2012; Liljedahl et al. 2019; Luukkonen et al. 2017; Wahlberg et al. 2019) and the contribution of CNV to dermal barrier function should be studied further.

The loss-of-function mutations included in our study are specific for European populations (Thyssen et al. 2014), except for R501X and 2282del4, which are found in other populations, including Korean and Japanese, however with lower frequencies (Park et al. 2015). The global combined allele frequency of the four mutations analyzed in our study is estimated to be between 0.0044 and 0.016, depending on which genome data set (1000 Genomes or gnomAD genomes) is used (<https://www.ensembl.org/>). It should be noted that the allele frequencies have been suggested to be underestimated in the 1000 Genomes database (Thyssen and Elias 2017). Non-European loss-of-function *FLG* mutations have been reported among Chinese, Japanese, and Korean populations (Park et al. 2015). One study identified 22 loss-of-function mutations in a study group of 425 Singaporean Chinese patients with atopic dermatitis, of which 20% had at least one mutation compared with 7% of the 440 controls (Chen et al. 2011). We therefore expect that there may be further, not yet identified, functional *FLG* mutations in other populations. Although *FLG* null had the largest impact on dermal absorption of chemicals, low CNV should also be considered a risk factor: it was associated with a higher uptake, faster lag time, and higher absorption rate of the chemicals under study. Low CNV is much more common, also in non-European populations, than null mutations. For example, one Korean study found a prevalence of low CNV (a total CNV of 20–22) of 36% among healthy participants after excluding the *FLG* null carriers (Li et al. 2016). Taken together, functional *FLG* variations vary in frequency between different populations, but *FLG* null and low CNV carriers are relatively common globally. Further research is needed to characterize the *FLG* variation and its impact on chemical uptake, particularly in non-European populations. At this time, better protection against dermal absorption of chemicals should be encouraged by appropriate legislation, for example by adjusting limit values for toxic substances in consumer products.

Associations between being a carrier of *FLG* null alleles and an increased risk of childhood atopic dermatitis and IgE-mediated allergies, such as allergic sensitization and allergic rhinitis, have been found (Palmer et al. 2006; van den Oord and Sheikh 2009). A low CNV has been associated with higher risk for atopic dermatitis (Brown et al. 2012). We did not find any associations between IgE-mediated allergies, cell-mediated allergies, or childhood or adult dermatitis and *FLG* genotype in this study, which could be a result of the relatively small study group

size and the fact that such symptoms are common in the population even without *FLG* null mutations (Ronmark et al. 2016; Theodosiou et al. 2019). Also, *FLG* null carriers with symptoms related to IgE-mediated allergies and dermatitis may be more likely to refrain from participating in a dermal exposure study, resulting in selection bias.

Variation in genes other than *FLG* could be relevant for the function of the skin barrier. However, compared with *FLG*, other genes have been much less studied in relation to skin disease. The epidermal differentiation complex on chromosome 1 is a cluster of genes of importance for skin cell function, such as skin cell differentiation and keratinocyte cornification. The epidermal differentiation complex includes, apart from *FLG*: *FLG2* [structure and function of the stratum corneum (Pendaries et al. 2015)], *GATA3* (a transcription factor for *FLG* and *FLG2*, (Zeitvogel et al. 2017)) and *SPRR3* [response to external insults to the skin (Cabral et al. 2001)], among others. Similar to that of *FLG*, genetic variation in these genes could possibly influence the function of the skin barrier and result in an increase in dermal absorption of chemicals.

Strengths of this study are that human subjects were used, that *FLG* genotype including CNV was taken into account, and that the dermal dose area and duration of the exposure were controlled. Other ways of performing skin absorption studies include using *in situ* modeling of skin absorption without experimental data, *in vivo* animal models, or *in vitro* skin models. None of these alternatives offer the complexity of being able to study skin absorption, distribution, metabolism, and excretion in human subjects, and they cannot be used to investigate the effect of genetic variation on skin absorption. Another strength of the study is that it includes healthy *FLG* null carriers, a group that has been little investigated because most research on *FLG* mutations has been performed in a clinical setting with patients with atopic dermatitis (Kezic and Jakasa 2016). Limitations of the study are that the selection of participants was based on the four most common *FLG* null mutations in Europe and that there is a risk that we missed very rare *FLG* mutations and mutations that are more common in other populations. However, all subjects but three (from other European countries) were from Sweden. We decided to group the participants according to both *FLG* null and total CNV. The *FLG* null and wt CNV20–22 groups were similar in size, but the wt CNV23–24 group was half the size of the other two groups, decreasing the statistical power to detect differences. Another limitation is that we could not distinguish which DNA strand carried the *FLG* null mutation, and hence we could not categorize the *FLG* null participants according to CNV, something which could have given information about extra-susceptible groups among the *FLG* null carriers. The skin barrier may have varying efficiency depending on the specific null mutations. However, due to the low numbers and the lack of CNV data for the functional allele among the null carriers, we could not investigate differences in  $AUC_{(0-40h)}$ , lag time, and absorption rate constant for specific genetic variation. Another limitation is that the model used to calculate lag times for absorption and absorption rates was more accurate for low than for high excretion rates (Figures S4–S6). A final limitation is that we analyzed only one gene in relation to skin absorption, and no other factors that could affect skin absorption, such as variation in other genes related to skin absorption or metabolism of the compounds, or the number of hair follicles present at the exposure site.

Our results show that *FLG* null carriers were more susceptible to dermal absorption of three common chemicals. Overall, *FLG* null carriers showed the shortest lag time for skin absorption, the highest rate constants for skin absorption, and higher fractions of the applied dose excreted. Further, our results indicate that low



CNV resulted in increased dermal absorption of the chemicals. Gaining knowledge about what *FLG* null mutations and CNV mean for dermal absorption is important to better understand skin barrier function and the preventive and protective measures and guidelines that should be implemented by authorities, caregivers, and employers to decrease skin exposure and skin absorption, such as imposing limit values for dermal exposure to consumer products and occupational chemicals and advising people to reduce their dermal exposure to certain chemicals.

## Acknowledgments

The authors thank all the study participants. The authors also thank H. Rastkhani for help with sample preparation and performing LC-MS/MS analysis. The project was funded by the Swedish Research Council for Health, Working Life and Welfare; Swedish Environmental Protection Agency; Swedish Research Council for Environment, Agricultural Sciences, and Spatial Planning; Karolinska Institutet, Region Skåne, and the Medical Faculty at Lund University.

## References

- Adoamnei E, Mendiola J, Moñino-García M, Vela-Soria F, Iribarne-Durán LM, Fernández MF, et al. 2018. Urinary concentrations of benzophenone-type ultra violet light filters and reproductive parameters in young men. *Int J Hyg Environ Health* 221(3):531–540, PMID: 29449081, <https://doi.org/10.1016/j.ijheh.2018.02.002>.
- Alhamedow A, Lindh C, Albin M, Gustavsson P, Tinnerberg H, Broberg K. 2017. Early markers of cardiovascular disease are associated with occupational exposure to polycyclic aromatic hydrocarbons. *Sci Rep* 7(1):9426, PMID: 28842704, <https://doi.org/10.1038/s41598-017-09956-x>.
- Anderson SE, Meade BJ. 2014. Potential health effects associated with dermal exposure to occupational chemicals. *Contact Dermatitis* 69(6):355–362, PMID: 23808934, <https://doi.org/10.1111/cod.12097>.
- Bandier J, Ross-Hansen K, Carlsen BC, Menné T, Linneberg A, Stender S, et al. 2013. Carriers of filaggrin gene (FLG) mutations avoid professional exposure to irritants in adulthood. *Contact Dermatitis* 69(6):355–362, PMID: 23808934, <https://doi.org/10.1111/cod.12097>.
- Blüthgen N, Zucchi S, Fent K. 2012. Effects of the UV filter benzophenone-3 (oxybenzone) at low concentrations in zebrafish (*Danio rerio*). *Toxicol Appl Pharmacol* 263(2):184–194, PMID: 22721600, <https://doi.org/10.1016/j.taap.2012.06.008>.
- Brown SJ, Kroboth K, Sandilands A, Campbell LE, Pohler E, Kezic S, et al. 2012. Intragenic copy number variation within filaggrin contributes to the risk of atopic dermatitis with a dose-dependent effect. *J Invest Dermatol* 132(1):98–104, PMID: 22071473, <https://doi.org/10.1038/jid.2011.342>.
- Brown SJ, McLean WHI. 2012. One remarkable molecule: filaggrin. *J Invest Dermatol* 132(3 Pt 2):751–762, PMID: 22158554, <https://doi.org/10.1038/jid.2011.393>.
- Cabral A, Voskamp P, Cleton-Jansen AM, South A, Nizetic D, Backendorf C. 2001. Structural organization and regulation of the small proline-rich family of cornified envelope precursors suggest a role in adaptive barrier function. *J Biol Chem* 276(22):19231–19237, PMID: 11279051, <https://doi.org/10.1074/jbc.M100336200>.
- Casarett LJ. 2001. *Absorption, Distribution, and Excretion of Toxicants in Casarett and Doull's Toxicology: The Basic Science of Poisons*. Klaassen, CD, ed. 6th ed. New York, NY: McGraw-Hill Medical Publishing Division.
- Chen H, Common JEA, Haines RL, Balakrishnan A, Brown SJ, Goh CSM, et al. 2011. Wide spectrum of filaggrin-null mutations in atopic dermatitis highlights differences between Singaporean Chinese and European populations. *Br J Dermatol* 165(1):106–114, PMID: 21428977, <https://doi.org/10.1111/j.1365-2133.2011.10331.x>.
- Ciarrocca M, Rosati MV, Tomei F, Capozzella A, Andreozzi G, Tomei G, et al. 2014. Is urinary 1-hydroxypyrene a valid biomarker for exposure to air pollution in outdoor workers? a meta-analysis. *J Expo Sci Environ Epidemiol* 24(1):17–26, PMID: 23299300, <https://doi.org/10.1038/jes.2012.111>.
- Faniband M, Ekman E, Littorin M, Maxe M, Larsson E, Lindh CH. 2019. Biomarkers of exposure to pyrimethanil after controlled human experiments. *J Anal Toxicol* 43(4):277–283, PMID: 30462228, <https://doi.org/10.1093/jat/bky091>.
- Golka K, Kopps S, Prager HM, Mende S, Thiel R, Jungmann O, et al. 2012. Bladder cancer in crack testers applying azo dye-based sprays to metal bodies. *J Toxicol Environ Health A* 75(8–10):566–571, <https://doi.org/10.1080/15287394.2012.675309>.
- Greisenegger E, Novak N, Maintz L, Bieber T, Zimprich F, Haubenberger D, et al. 2010. Analysis of four prevalent filaggrin mutations (R501X, 2282del4, R2447X and S3247X) in Austrian and German patients with atopic dermatitis. *J Eur Acad Dermatol Venereol* 24(5):607–610, PMID: 19874431, <https://doi.org/10.1111/j.1468-3083.2009.03469.x>.
- Han C, Lim YH, Hong YC. 2016. Ten-year trends in urinary concentrations of triclosan and benzophenone-3 in the general U.S. population from 2003 to 2012. *Environ Pollut* 208(Pt B):803–810, PMID: 26602792, <https://doi.org/10.1016/j.envpol.2015.11.002>.
- Hurley PM. 1998. Mode of carcinogenic action of pesticides inducing thyroid follicular cell tumors in rodents. *Environ Health Perspect* 106(8):437–445, PMID: 9681970, <https://doi.org/10.1289/ehp.98106437>.
- Joensen UN, Jørgensen N, Meldgaard M, Frederiksen H, Andersson A-M, Menné T, et al. 2014. Associations of filaggrin gene loss-of-function variants with urinary phthalate metabolites and testicular function in young Danish men. *Environ Health Perspect* 122(4):345–350, PMID: 24380925, <https://doi.org/10.1289/ehp.1306720>.
- Joensen UN, Jørgensen N, Thyssen JP, Petersen JH, Szecsi PB, Stender S, et al. 2017. Exposure to phenols, parabens and UV filters: associations with loss-of-function mutations in the filaggrin gene in men from the general population. *Environ Int* 105:105–111, PMID: 28525834, <https://doi.org/10.1016/j.envint.2017.05.013>.
- Kammer R, Tinnerberg H, Eriksson K. 2011. Evaluation of a tape-stripping technique for measuring dermal exposure to pyrene and benzo(a)pyrene. *J Environ Monit* 13(8):2165–2171, PMID: 21687840, <https://doi.org/10.1039/c1em10245a>.
- Kezic S, Jakasa I. 2016. Filaggrin and skin barrier function. *Curr Probl Dermatol* 49:1–7, PMID: 26844893, <https://doi.org/10.1159/000441539>.
- Law FC, Meng JX, He YT, Chui YC. 1994. Urinary and biliary metabolites of pyrene in rainbow trout (*Oncorhynchus mykiss*). *Xenobiotica* 24(3):221–229, PMID: 8009885, <https://doi.org/10.3109/00498259409043234>.
- Li K, Seok J, Park KY, Yoon Y, Kim KH, Seo SJ. 2016. Copy-number variation of the filaggrin gene in Korean patients with atopic dermatitis: what really matters, 'number' or 'variation'? *Br J Dermatol* 174(5):1098–1100, PMID: 26554544, <https://doi.org/10.1111/bjd.14287>.
- Liljedahl ER, Wahlberg K, Lidén C, Albin M, Broberg K. 2019. Genetic variants of filaggrin are associated with occupational dermal exposure and blood DNA alterations in hairdressers. *Sci Total Environ* 653:45–54, PMID: 30399560, <https://doi.org/10.1016/j.scitotenv.2018.10.328>.
- Luukkonen TM, Kiiski V, Ahola M, Mandelin J, Virtanen H, Pöyhönen M, et al. 2017. The value of FLG null mutations in predicting treatment response in atopic dermatitis: an observational study in Finnish patients. *Acta Derm Venereol* 97(4):456–463, PMID: 27840886, <https://doi.org/10.2340/00015555-2578>.
- Mazzachi BC, Peake MJ, Ehrhardt V. 2000. Reference range and method comparison studies for enzymatic and Jaffé creatinine assays in plasma and serum and early morning urine. *Clin Lab* 46(1–2):53–55, PMID: 10745982.
- Medjakovic S, Zoehling A, Gerster P, Ivanova MM, Teng Y, Klinge CM, et al. 2014. Effect of nonpersistent pesticides on estrogen receptor, androgen receptor, and aryl hydrocarbon receptor. *Environ Toxicol* 29(10):1201–1216, PMID: 23436777, <https://doi.org/10.1002/tox.21852>.
- Nakano M, Omae K, Takebayashi T, Tanaka S, Koda S. 2018. An epidemic of bladder cancer: ten cases of bladder cancer in male Japanese workers exposed to ortho-toluidine. *J Occup Health* 60(4):307–311, PMID: 29743389, <https://doi.org/10.1539/joh.2017-0220-OA>.
- Nielsen JB, Sørensen JA, Nielsen F. 2009. The usual suspects—influence of physicochemical properties on lag time, skin deposition, and percutaneous penetration of nine model compounds. *J Toxicol Environ Health A* 72(5):315–323, PMID: 19184747, <https://doi.org/10.1080/15287390802529872>.
- Okereke CS, Kadry AM, Abdel-Rahman MS, Davis RA, Friedman MA. 1993. Metabolism of benzophenone-3 in rats. *Drug Metab Dispos* 21(5):788–791, PMID: 7902237.
- Paggiaro PL, Bacci E, Dente FL, Talini D, Giuntini C. 1987. Prognosis of occupational asthma induced by isocyanates. *Bull Eur Physiopathol Respir* 23(6):565–569, PMID: 3331124.
- Palmer CN, Irvine AD, Terron-Kwiatkowski A, Zhao Y, Liao H, Lee SP, et al. 2006. Common loss-of-function variants of the epidermal barrier protein filaggrin are a major predisposing factor for atopic dermatitis. *Nat Genet* 38(4):441–446, PMID: 16550169, <https://doi.org/10.1038/ng1767>.
- Park J, Jekarl DW, Kim Y, Kim J, Kim M, Park YM. 2015. Novel FLG null mutations in Korean patients with atopic dermatitis and comparison of the mutational spectra in Asian populations. *J Dermatol* 42(9):867–873, PMID: 25997159, <https://doi.org/10.1111/1346-8138.12935>.
- Pendaries V, Le Lamer M, Cau L, Hansmann B, Malaisse J, Kezic S, et al. 2015. In a three-dimensional reconstructed human epidermis filaggrin-2 is essential for proper cornification. *Cell Death Dis* 6(2):e1656–e1656, PMID: 25695608, <https://doi.org/10.1038/cddis.2015.29>.
- Petsonk EL, Wang ML, Lewis DM, Siegel PD, Husberg BJ. 2000. Asthma-like symptoms in wood product plant workers exposed to methylene diphenyl diisocyanate. *Chest* 118(4):1183–1193, PMID: 11035694, <https://doi.org/10.1378/chest.118.4.1183>.
- Potts RO, Guy RH. 1992. Predicting skin permeability. *Pharm Res* 9(5):663–669, PMID: 1608900, <https://doi.org/10.1023/A:1015810312465>.

- PubChem. 2004a. PubChem Compound Summary for CID 31423, Pyrene. <https://pubchem.ncbi.nlm.nih.gov/compound/Pyrene> [accessed 19 November 2020].
- PubChem. 2004b. PubChem Compound Summary for CID 4632, Oxybenzone. <https://pubchem.ncbi.nlm.nih.gov/compound/4632> [accessed 19 November 2020].
- PubChem. 2004c. PubChem Compound Summary for CID 91650, Pyrimethanil. <https://pubchem.ncbi.nlm.nih.gov/compound/Pyrimethanil> [accessed 19 November 2020].
- Redlich CA. 2010. Skin exposure and asthma: is there a connection? *Proc Am Thorac Soc* 7(2):134–137, PMID: 20427586, <https://doi.org/10.1513/pats.201002-025RM>.
- Ronmark E, Backman H, Hedman L. 2016. Allergies are the largest disease group of Swedish children and young adults. *Läkartidningen* 113:DWF4, PMID: 27046755.
- Roskams N, Op de Beeck R, De Craecker W. 2008. Occupational skin diseases and dermal exposure in the European Union (EU-25): Policy and practice overview. European Agency for Safety and Health at Work, <https://doi.org/10.2802/15493> [accessed 19 November 2020].
- Saengtienchai A, Ikenaka Y, Nakayama SM, Mizukawa H, Kakehi M, Bortey-Sam N, et al. 2014. Identification of interspecific differences in phase II reactions: determination of metabolites in the urine of 16 mammalian species exposed to environmental pyrene. *Environ Toxicol Chem* 33(9):2062–2069, PMID: 24899081, <https://doi.org/10.1002/etc.2656>.
- Sandilands A, Sutherland C, Irvine AD, McLean WH. 2009. Filaggrin in the frontline: role in skin barrier function and disease. *J Cell Sci* 122(Pt 9):1285–1294, PMID: 19386895, <https://doi.org/10.1242/jcs.033969>.
- Sandilands A, Terron-Kwiatkowski A, Hull PR, O'Regan GM, Clayton TH, Watson RM, et al. 2007. Comprehensive analysis of the gene encoding filaggrin uncovers prevalent and rare mutations in ichthyosis vulgaris and atopic eczema. *Nat Genet* 39(5):650–654, PMID: 17417636, <https://doi.org/10.1038/ng2020>.
- Santamaria CG, Meyer N, Schumacher A, Zenclussen ML, Teglia CM, Culzoni MJ, et al. 2020. Dermal exposure to the UV filter benzophenone-3 during early pregnancy affects fetal growth and sex ratio of the progeny in mice. *Arch Toxicol* 94(8):2847–2859, PMID: 32430675, <https://doi.org/10.1007/s00204-020-02776-5>.
- Smith FJ, Irvine AD, Terron-Kwiatkowski A, Sandilands A, Campbell LE, Zhao Y, et al. 2006. Loss-of-function mutations in the gene encoding filaggrin cause ichthyosis vulgaris. *Nat Genet* 38(3):337–342, PMID: 16444271, <https://doi.org/10.1038/ng1743>.
- Strandberg B, Julander A, Sjöström M, Lewné M, Hatice KA, Bigert C. 2018. An improved method for determining dermal exposure to polycyclic aromatic hydrocarbons. *Chemosphere* 198:274–280, PMID: 29421739, <https://doi.org/10.1016/j.chemosphere.2018.01.104>.
- Theodosiou G, Montgomery S, Metsini A, Dalgard FJ, Svensson A, Kobyletzki LB. 2019. Burden of atopic dermatitis in Swedish adults: a population-based study. *Acta Derm Venereol* 99(11):964–970, PMID: 31289842, <https://doi.org/10.2340/00015555-3257>.
- Thyssen JP, Bikle DD, Elias PM. 2014. Evidence that loss-of-function filaggrin gene mutations evolved in northern Europeans to favor intracutaneous vitamin D<sub>3</sub> production. *Evol Biol* 41(3):388–396, PMID: 25506102, <https://doi.org/10.1007/s11692-014-9282-7>.
- Thyssen JP, Elias PM. 2017. It remains unknown whether filaggrin gene mutations evolved to increase cutaneous synthesis of vitamin D. *Genome Biol Evol* 9(4):900–901, PMID: 28338939, <https://doi.org/10.1093/gbe/evx049>.
- Uter W, Gonçalo M, Yazar K, Kratz EM, Mildau G, Lidén C. 2014. Coupled exposure to ingredients of cosmetic products: III. ultraviolet filters. *Contact Dermatitis* 71(3):162–169, PMID: 24761783, <https://doi.org/10.1111/cod.12245>.
- van den Oord RA, Sheikh A. 2009. Filaggrin gene defects and risk of developing allergic sensitisation and allergic disorders: systematic review and meta-analysis. *BMJ* 339:b2433, PMID: 19589816, <https://doi.org/10.1136/bmj.b2433>.
- Varbo A, Nordestgaard BG, Benn M. 2017. Filaggrin loss-of-function mutations as risk factors for ischemic stroke in the general population. *J Thromb Haemost* 15(4):624–635, PMID: 28164424, <https://doi.org/10.1111/jth.13644>.
- Visser MJ, Landeck L, Campbell LE, McLean WHI, Weidinger S, Calkoen F, et al. 2013. Impact of atopic dermatitis and loss-of-function mutations in the filaggrin gene on the development of occupational irritant contact dermatitis. *Br J Dermatol* 168(2):326–332, PMID: 23039796, <https://doi.org/10.1111/bjd.12083>.
- Wahlberg K, Liljedahl ER, Alhamdow A, Lindh C, Lidén C, Albin M, et al. 2019. Filaggrin variations are associated with PAH metabolites in urine and DNA alterations in blood. *Environ Res* 177:108600, PMID: 31369996, <https://doi.org/10.1016/j.envres.2019.108600>.
- World Health Organization. 2014. Dermal exposure (Environmental Health Criteria 242). [https://www.who.int/ipcs/publications/ehc/ehc\\_242.pdf?ua=1](https://www.who.int/ipcs/publications/ehc/ehc_242.pdf?ua=1) [accessed 19 November 2020].
- Zeitvogel J, Jokmin N, Rieker S, Klug I, Brandenberger C, Werfel T. 2017. GATA3 regulates FLG and FLG2 expression in human primary keratinocytes. *Sci Rep* 7(1):11847, PMID: 28928464, <https://doi.org/10.1038/s41598-017-10252-x>.